

# Enhanced ionic conductivity of anion exchange membranes by grafting flexible ionic strings on multiblock copolymers

 The corrections made in this section will be reviewed and approved by journal production editor.

Ao Nan **Lai**<sup>a,\*</sup> [aonanlai@hqu.edu.cn](mailto:aonanlai@hqu.edu.cn), Yi Zhi **Zhuo**<sup>b</sup>, Peng Cheng **Hu**<sup>a</sup>, Jing Wei **Zheng**<sup>a</sup>, Shu Feng **Zhou**<sup>a</sup>,  
Lei **Zhang**<sup>c</sup>

<sup>a</sup>College of Chemical Engineering, Huaqiao University, Xiamen, 361021, PR China

<sup>b</sup>NTNU Nanomechanical Lab, Department of Structural Engineering, Norwegian University of Science and Technology (NTNU), Trondheim, 7491, Norway

<sup>c</sup>College of Materials Science and Engineering, Fujian University of Technology, Fuzhou, 350118, PR China

\* *Corresponding author.*

---

## Abstract

A new strategy to prepare high-conductivity anion exchange membranes (AEMs) is presented here. A series of phenolphthalein-based poly(arylene ether sulfone nitrile) multiblock AEMs has been synthesized by selectively grafting flexible ionic strings on hydrophilic segments to form ionic regions. Moreover, the phenolphthalein groups are introduced to force chains apart and create additional interchain spacing. In addition, the nitrile groups suspended on main chains are aimed at enhancing the anti-swelling behavior of as-prepared AEMs. Along these processes, well-defined phase separation has been attained, forming excellent ion-transport channels. The effective phase separation has been confirmed by atomic force microscopy. Finally, as-prepared AEMs exhibit a high hydroxide conductivity, ranging from 40.1 to 121.6 mS cm<sup>-1</sup> in the temperature range of 30–80 °C, and superior ionic conductivity to IEC ratio at 80 °C. Furthermore, excellent thermal stability and desirable mechanical strength have been rendered by as-prepared AEMs. However, the alkaline stability of as-prepared AEMs requires further optimization.

---

**Keywords:** Anion exchange membrane; Ionic strings; Multiblock copolymers; Phenolphthalein group; Hydroxide conductivity

## Introduction

In the past decades, polymer electrolyte fuel cells (PEFCs) have received great attention owing to their high efficiency, superior energy density, utilization of renewable fuels and environment-friendly exhaust [1–3]. As the most common type of PEFCs, proton exchange membrane fuel cells (PEMFCs) based on acidic polyelectrolyte have been broadly researched [4]. However, the high cost of precious metal catalysts, predominantly platinum (Pt) and proton exchange membranes, such as Nafion<sup>®</sup>, hinders the widespread commercialization of PEMFCs [5,6]. Anion exchange membrane fuel cells (AEMFCs), which are operated in basic conditions, are being developed as an alternative in terms of the faster oxygen reduction kinetics together with potential utilization of non-precious metals as catalysts, such as cobalt (Co) and nickel (Ni) [7,8]. Hence, the overall cost of PEFCs shall be significantly reduced.

As one of the key components in AEMFCs, anion exchange membranes (AEMs) should prevent the crossover of oxidant and fuel and transfer anions from cathode to anode. Polymers such as poly(arylene ether sulfone) [9,10], poly(ether imide) [11], poly(phenylene oxide) [12], polymerized ionic liquid [13,14], poly(styrene)s [15] and poly(arylene ether ketone) [16] have been used to prepare AEMs by incorporating with cationic functional groups, such as quaternary ammonium [10–12], sulfonium [9], imidazolium [13–15], guanidinium [17] and metal cations [18]. However, current AEMs suffer from insufficient stability and ionic conductivity, limiting their applications in AEMFCs [19,20]. The ionic conductivity can be improved by increasing the ion exchange capacity (IEC) of AEMs. However, high IEC of AEMs tend to swell seriously and weaken the dimensional stability, resulting in a decrease in mechanical strength and failure in practical applications.

Recently, it has been demonstrated that well-defined microphase-separated membrane structures can promote the construction of ionic conductive channels and improve hydroxide conductivity [21–23]. Hence, several “block-type” AEMs have been prepared by incorporating alkaline functional groups on the hydrophilic segments of block copolymers [24–29]. These AEMs exhibit obvious hydrophilic/hydrophobic microphase structure and possess relatively high conductivity. Another effective approach to improve the microphase separation is to construct “side-chain-type” AEMs, bearing ion-conducting groups on side chains, which are separated from polymer main chains [30–34]. Previously, we have reported a series of phenolphthalein-based poly(arylene ether sulfone nitrile) side-chain-type AEMs, with imidazolium groups on the pendent stiff cardo rings, and demonstrated a well-defined microphase-separated structure with a maximum hydroxide conductivity of 81.4 mS cm<sup>-1</sup> at 80 °C (IEC = 1.35 meq g<sup>-1</sup>) [32]. Furthermore, a set of novel side-chain-type AEMs, possessing flexible side chains, have been developed to enhance the mobility of ion-conducting groups [35–39]. In these AEMs, the ionic groups tend to self-assemble and form larger ionic clusters, which can enhance the microphase separation ability and anion conductivity. For instance, FPAES-Im-x AEMs exhibited favorable hydroxide conductivity, ranging from 48.5 to 83.1 mS cm<sup>-1</sup> at 80 °C with IEC of 1.35–1.92 meq g<sup>-1</sup> [37]. Recently, some “ionic string-type” AEMs, with multiple ion-conducting groups on flexible side chains, have been reported to further enhance the aggregation of ionic conductive groups for high performance [40–42].

Herein, inspired by appealing characteristics of the above mentioned architectures, we aimed to combine the advantages of block-type and ionic string-type structures to construct high-performance AEMs. In this study, a quaternization reagent, with a quaternary ammonium cation and a tertiary ammonium group on a single chain, has been synthesized by reacting bromoethane with N,N,N',N'-tetramethyl-1,6-hexanediamine (TMHDA). Meanwhile, a series of tetramethyl-containing phenolphthalein-based poly(arylene ether sulfone nitrile) multiblock copolymers have been synthesized, further brominated and quaternization to fabricate AEMs. Along these processes, a single ionic string side chain has been charged with two quaternary ammonium cations and selectively grafted on the tetramethyl-phenolphthalein unit as hydrophilic segment, facilitating the construction of phase-separated structure and ion-transport channels. Furthermore, phenolphthalein groups, which containing rigid and bulk cardo groups, have also been introduced to force chains apart and generate additional interchain spacing for water storage and OH<sup>-</sup> transport [43]. In addition, nitrile groups with strong polar were introduced to enhance the dimensional stability of membranes [43,44]. Then, the influence of ionic strings content has been systematically investigated by structure–property analysis.

## Experimental

### Materials

TMHDA (98.0%, TCI, Japan), bromoethane (99.0%, Adamas, China), phenolphthalein (98%, Sigma-Aldrich, USA), toluene (99.8% HPLC, Adamas, China), 2,6-difluorobenzonitrile (DFBN, 99%, TCI, Japan), N,N-dimethylacetamide (DMAc, 99.8% SafeDry, Adamas, China), dimethyl sulfoxide (DMSO, 99.7% SafeDry, Adamas, China) and N-bromosuccinimide (NBS, 99%, Aladdin, China) were used as received. Benzoyl peroxide (BPO, 97%, Alfa Aesar, UK) was purified by chloroform-assisted recrystallization. All other reagents were obtained from Sinopharm Group Chemical Reagent and used directly.

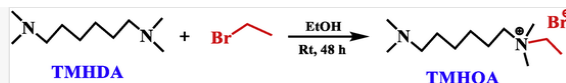
### Preparation of AEMs

#### Synthesis of 6-(dimethylamino)-N-ethyl-N,N-dimethylhexan-1-aminium bromide (TMHQA) monomer

TMHQA was synthesized from TMHDA and bromoethane (Scheme 1), as described elsewhere [40]. Briefly, TMHDA (6.4 mL, 30 mmol), bromoethane (1.5 mL, 20 mmol) and 50 mL ethanol were added into a 150 mL three-necked flask. The mixture was stirred at room temperature (RT) for 48 h under nitrogen. Then, the ethanol was removed using a rotary evaporator and residues were poured into 30 mL diethyl ether to get a precipitate. The precipitate was filtered and thoroughly washed with acetone, followed by vacuum drying at 60 °C for 24 h. The as-obtained product was recrystallized from acetone/diethyl ether mixture (1:1), resulting in pure TMHQA (yield: 61%).

alt-text: Scheme 1

Scheme 1



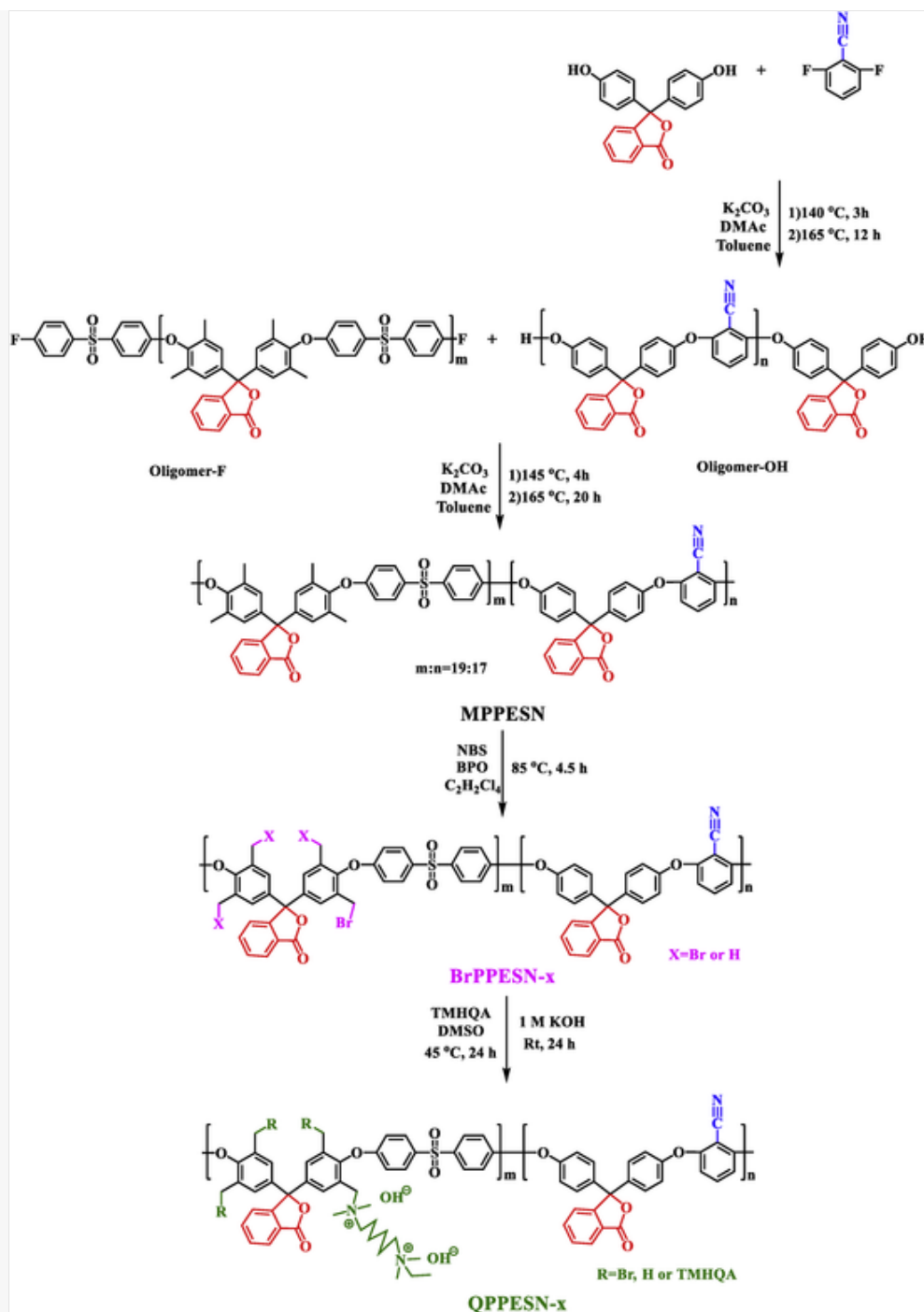
Synthesis of TMHQA.

### Synthesis of hydroxy-terminated telechelic oligomer(oligomer-OH)

The oligomer-OH was prepared through polycondensation reaction, as shown in [Scheme 2](#). In a typical reaction, a 150 mL three-necked flask equipping with a Dean-Stark trap, a magnetic stirrer and a gas inlet was charged with phenolphthalein (3.3424 g, 10.5 mmol), DFBN (1.3910 g, 10 mmol),  $\text{K}_2\text{CO}_3$  (3.4553 g, 25 mmol), 30 mL DMAc and 15 mL toluene. Under  $\text{N}_2$  atmosphere, the mixture was refluxed at 140 °C for 3 h and at 165 °C for another 12 h. Finally, additional 10 mg phenolphthalein was added to assure the end-capping. After cooled at RT, the mixture was precipitated in 60 °C methanol/water (350 mL,  $v/v = 1/1$ ) solution. The obtained copolymer was kept stirring for 4 h, filtered, followed by Soxhlet extracting for another 6 h with methanol. Then a white-colored solid product was obtained after vacuum drying at 65 °C for 24 h. Moreover, the oligomer-F was prepared as previous described [\[43\]](#).

alt-text: Scheme 2

Scheme 2



Synthesis process of oligomer-OH, MPPESEN, BrPPESN-x and QPPESN-x.

## Synthesis of multiblock phenolphthalein-based poly(arylene ether sulfone nitrile) (MPPESEN)

The typical process of MPPESEN synthesis is schematically illustrated in Scheme 2. Briefly, equimolar amounts of oligomer-OH and oligomer-F were mixed with DMAC, toluene and  $K_2CO_3$ , and reacted at 145 °C for 4 h and at 165 °C for another 20 h under  $N_2$  atmosphere. Finally, the reaction solution was diluted by additional DMAC. The mixture was poured into a methanol aqueous solution and collected by filtration. Then, the as-obtained copolymer was washed repeatedly using methanol by Soxhlet extracting and dried at 65 °C under vacuum to attain MPPESEN.

## Bromination of MPPESEN

The bromination reaction of MPPESEN is shown in [Scheme 2](#). In general, 2 g of MPPESEN (containing 8.43 mmol of  $-\text{CH}_3$ ) was dissolved in 25 mL of 1,1,2,2-tetrachloroethane (TCE) under stirring. Then, 0.046 g of BPO (0.19 mmol) and 0.675 g of NBS (3.79 mmol) were added into the above mixture. The mixture was reacted at 85 °C for 4.5 h in a  $\text{N}_2$  atmosphere. Then the reaction solution was dropped into a methanol solution (300 mL). The obtained precipitate was collected and washed by using a Soxhlet extractor, followed by vacuum drying at 65 °C, which resulted in a yellow solid of BrPPESN-2, where Br represents the bromination reaction. In addition, BrPPESN- $x$ , with different bromination degrees, was synthesized by varying the feeding ratio of NBS to MPPESEN.

## Synthesis of quaternized phenolphthalein-based poly(arylene ether sulfone nitrile) (QPPESEN- $x$ ) and membrane preparation

Quaternization of BrPPESN- $x$  was performed by using TMHQA as quaternization reagent ([Scheme 2](#)). Briefly, 1 g of BrPPESN-2 (containing 1.26 mmol of  $-\text{CH}_2\text{Br}$ ) was dissolved in 20 mL of DMSO under agitation. Subsequently, 0.421 g of TMHQA (1.5 mmol) was slowly added into the above mixture. The solution was kept stirring at 45 °C for 24 h, then filtered by a PTFE microporous (0.45  $\mu\text{m}$ ) filter, cast on a glass substrate and dried at 65 °C for 36 h under vacuum. The as-obtained membranes were soaked in KOH aqueous solution (1 mol  $\text{L}^{-1}$ ) for ion exchange and kept in deionized water before use. During this period, the AEMs, KOH solution and the deionized water were kept in a chamber which was charged with flowing  $\text{N}_2$  gas for protecting from air. The as-prepared AEMs, with a thickness of  $\sim 30 \mu\text{m}$ , were termed QPPESEN-2, where Q denotes the quaternization.

## Characterization

### $^1\text{H}$ NMR, FT-IR and GPC

$^1\text{H}$  NMR spectra were obtained on a Bruker Avance III spectrometer (500 MHz).  $\text{DMSO-}d_6$  or  $\text{CDCl}_3$  were used as deuterated solvents. FT-IR spectra were received by using a Thermo Scientific Nicolet iS50 with an accumulation of 32 scans in the range 500–4000  $\text{cm}^{-1}$ . GPC analysis was conducted on a Waters 1515 system, where polystyrene was used as a standard and tetrahydrofuran (THF, HPLC grade) as an eluent (1.0 ml  $\text{min}^{-1}$ ).

### Ion exchange capacity (IEC)

A back-titration method was used to measure the IEC of QPPESEN- $x$  AEMs. First, the  $\text{OH}^-$  formed AEMs were vacuum dried at 65 °C for 36 h, then soaked into HCl solution (0.1 mol  $\text{L}^{-1}$ ) for 48 h. Subsequently, the back-titration was carried out by using standard KOH solution (0.05 mol  $\text{L}^{-1}$ ). The IEC value ( $\text{meq g}^{-1}$ ) was calculated by using Equation (1):

$$IEC = \frac{M_{o,HCl} - M_{e,HCl}}{md} \times 100\%$$

(1)

where  $m_d$  (g) represents the mass of the dried membrane, and  $M_{o,HCl}$  and  $M_{e,HCl}$  (meq) refer to the milliequivalents of HCl before and after equilibrium, respectively.

### Water uptake (WU) and swelling ratio (SR)

To assess the WU and SR, the OH<sup>-</sup> form AEMs in square shape were soaked into deionized water for 24 h at various temperatures. During this period, the AEMs and deionized water were kept in a chamber which was charged with flowing N<sub>2</sub> gas for protecting from air. After being wiped with filter papers, the size ( $L_{wet}$ ) and weight ( $M_{wet}$ ) of the hydrated membrane was recorded quickly. Subsequently, the membrane was vacuum dried at 65 °C for 36 h to record the corresponding size ( $L_{dry}$ ) and weight ( $M_{dry}$ ) of dried membrane. Then, Equations (2) and (3) were used to calculate WU and SR, respectively.

$$WU = \frac{M_{wet} - M_{dry}}{M_{dry}} \times 100\% \quad (2)$$

$$SR = \frac{L_{wet} - L_{dry}}{L_{dry}} \times 100\% \quad (3)$$

The hydrated number ( $\lambda$ ) represents the amount of absorbed H<sub>2</sub>O per functional group and can be determined by Equation (4):

$$\lambda = \frac{WU}{18.02} \times \frac{1000}{IEC} \quad (4)$$

### Atomic force microscopy (AFM) and ionic conductivity

The AFM morphology of AEMs was observed by using AFM5500 (Agilent Technologies, Inc.) under ambient conditions and tapping mode. Prior to AFM observations, the samples were equilibrated at 25 °C and 60% relative humidity (RH) for 24 h.

A two-electrode AC impedance spectroscopy method was used to measure the resistance of the membranes on a Parstat 2273 electrochemical system (Ametek Inc., USA). The testing was performed on the OH<sup>-</sup> form membranes in deionized water at various temperatures from 30 °C to 80 °C in a chamber. The chamber was charged with flowing N<sub>2</sub> gas during the measurement. The hydroxide conductivity values ( $\sigma$ , mS·cm<sup>-1</sup>) were calculated by using Equation (5):

$$\sigma = \frac{1}{R} \times \frac{L}{A} \quad (5)$$

$$\sigma = \frac{l}{RA}$$

(5)

where  $l$  (cm) refers to the measured distance of the adjacent electrodes,  $R$  ( $\Omega$ ) and  $A$  ( $\text{cm}^2$ ) refers to the resistance and cross-sectional area of the membrane, respectively.

### **Mechanical characterization, thermal and alkaline stability**

The mechanical property of each membrane was measured at 25 °C and 60% RH with a stretching speed of 5 mm min<sup>-1</sup> by using WD-300K universal material testing system. Prior to testing, the membranes, with a width of 15 mm, were kept in deionized water at 25 °C for 24 h.

The thermal stability was assessed by carrying out thermogravimetric analysis (TGA, SHIMADZU DTG-60H) under N<sub>2</sub> atmosphere at a heating rate of 10 °C·min<sup>-1</sup>. Prior to thermogravimetric analysis, the membranes were vacuum dried at 65 °C for 36 h.

The alkaline stability was examined at 80 °C for 360 h by soaking the membrane (OH<sup>-</sup> form) in KOH aqueous solution (1 mol L<sup>-1</sup>). During this period, the solution was kept in a chamber which was charged with flowing N<sub>2</sub> gas for protecting from air. The change in IEC and ionic conductivity of the membranes has been investigated during the immersion period.

### **Single cell assembly and measurement**

An ionomer solution of QPPESN-2 (5 wt% in DMF) was sprayed onto a 4 cm<sup>2</sup> catalyst-loaded carbon paper (1 mg cm<sup>-2</sup> Pt, Johnson Matthey Co.) to prepare the electrodes and diffusion layer. The membrane electrode assembly (MEA) was prepared by sandwiching the QPPESN-2 membrane between two pieces of carbon papers and hot-pressing at 60 °C and 0.5 MPa for 8 min. The H<sub>2</sub>/O<sub>2</sub> single cell measurement was conducted on a fuel cell test system (TE201, Kunshan Sunlaite, China) with O<sub>2</sub> (cathode, 100 mL min<sup>-1</sup>) and H<sub>2</sub> (anode, 100 mL min<sup>-1</sup>) at 80 °C under 100% RH.

## **Results and discussion**

### **Synthesis and characterization of TMHQA and oligomer-OH**

TMHQA was synthesized by reacting bromoethane with TMHDA in ethanol at RT for 48 h and the chemical structure was characterized by <sup>1</sup>H NMR. As shown in Fig. S1 (supporting information), the signals at 2.15 and 2.96 ppm can be ascribed to the methyl of tertiary amine and quaternary ammonium, respectively. By comparing the integrated areas of the above two peaks (peaks 1 and 8 in Fig. S1), the chemical structure of TMHQA with a tertiary ammonium group and a quaternary ammonium cation on a single chain was confirmed. The signals at 2.31 and 3.19 ppm can be assigned to the methylene adjacent the tertiary amine and quaternary ammonium, respectively. The peaks at ~1.32, 1.44 and 1.70 ppm can be indexed to other methylene protons on TMHQA. The peak at 4.70 ppm can be assigned to D<sub>2</sub>O. The successful synthesis of TMHQA is thus confirmed.



The oligomer–OH was synthesized through polycondensation reactions and the chemical structure was characterized by using  $^1\text{H}$  NMR. As shown in Fig. S2 (supporting information), the signals at 7.45 and 7.24 ppm can be associated with oxy-phenylene rings protons (Hi and Hj), whereas the peaks at 7.08 and 6.77 ppm can be associated with OH–terminated phenylene rings (Hi' and Hj'), which appears at higher magnetic fields by an electron-donating effect of hydroxyl groups. These analyses suggest the successful synthesis of oligomer–OH. The polymerization degree of oligomer–OH was  $n = 17$  from GPC (Table S1, supporting information). The synthesis of oligomer–F is described elsewhere [43] and the polymerization degree was found to be  $m = 19$ .

## Synthesis and characterization of MPPESEN and BrPPESEN- $x$

Block copolymers (MPPESEN) were synthesized through the copolycondensation reaction. The  $^1\text{H}$  NMR spectrum of MPPESEN is presented in Fig. S3(a) (supporting information). The signals at  $\sim 2.05$  ppm can be ascribed to the protons of benzylmethyl groups on hydrophilic segments ( $a$  in Fig. S3(a)) of MPPESEN. The characteristic signals of phenolphthalein group have been observed at 7.99, 7.78 and 7.66–7.58 ppm ( $b$ ,  $c$ ,  $d$  and  $e$  in Fig. S3(a)), respectively. In addition, the other signals can be well-assigned to the aimed copolymer structure, and the end–group peaks assigned to the telechelic oligomers disappear. These results confirm the successful synthesis of the target block copolymers. Furthermore, MPPESEN shows a sufficient molecular weight ( $M_n > 84$  kDa, Table S1) for membrane formation.

The brominated block copolymers (BrPPESEN- $x$ ) were prepared through bromomethylation reaction. Fig. S3(b) (supporting information) presents  $^1\text{H}$ NMR spectrum of BrPPESEN-2 as a typical example. A comparison between Fig. S3 (a) and (b) illustrates that new clear signals around 4.18–4.35 ppm can be ascribed to bromomethyl groups ( $a'$  in Fig. S3(b)), and the related signals of benzylmethyl groups decreased in size ( $a$  in Fig. S3). These results confirm the successful conduct of bromination reaction. The bromination degree can be given as: Bromination degree =  $3S_1/(3S_1+2S_2)$ , where  $S_1$  represents the integrated area of bromomethyl groups ( $-\text{CH}_2\text{Br}$ , two protons) and  $S_2$  represents the integrated area of remained benzylmethyl groups ( $-\text{CH}_3$ , three protons). Then the bromination degree of BrPPESEN- $x$  was found to be ca. 22.6%, 33.1% and 41.5% at  $x = 1, 2$  and  $3$ , respectively, as summarized in Table 1.

alt-text: Table 1

Table 1



The presentation of Tables and the formatting of text in the online proof do not match the final output, though the data is the same. To preview the actual presentation, view the Proof.

Key properties of BrPPESEN- $x$  and QPPESEN- $x$  AEMs.

BrPPESEN- $x$	Bromination degree (%) <sup>a</sup>	AEMs	IEC (meq g <sup>-1</sup> )		$\lambda^d$		
			Theo. <sup>b</sup>	Exp. <sup>c</sup>	30 °C	60 °C	80 °C
BrPPESEN-1	22.6%	QPPESEN-1	1.54	1.37	10.7	11.8	12.7

BrPPESN-2	35.1%	QPPESEN-2	2.17	1.86	11.2	12.8	14.1
BrPPESN-3	44.5%	QPPESEN-3	2.58	2.12	11.6	14.3	15.6

#### Table Footnotes

<sup>a</sup>Calculated from <sup>1</sup>H NMR spectra.

<sup>b</sup>Determined from bromination degree and composition of BrPPESN-*x*.

<sup>c</sup>Measured by back-titration method, and.

<sup>d</sup>Calculated from Exp. IECs and WU of AEMs.

## Membrane formation and FT-IR spectrum

The QPPESEN-*x* membranes were prepared by using BrPPESN-*x* as the base copolymers, and TMHQA as a quaternization reagent. <sup>1</sup>H NMR spectrum of QPPESEN-2 (Fig. S4, supporting information) clearly shows characteristic peaks at ~4.65 ppm and 2.97 ppm, which can be associated with protons of N-CH<sub>2</sub>-Ar (*a''* in Fig. S4) and N-CH<sub>3</sub> (*H<sub>1</sub>* in Fig. S4), respectively. In addition, the other characteristic peaks from H<sub>2</sub> to H<sub>5</sub> can be assigned to methyl and methylene protons of TMHQA, confirming the successful introduction of TMHQA into AEMs.

The chemical structure of QPPESEN-*x* was further determined by FT-IR spectroscopy. Fig. S5 (Supporting information) presents FT-IR spectra of BrPPESN-2 and QPPESEN-2. The characteristic signals at 2227 cm<sup>-1</sup> and 1240 cm<sup>-1</sup> can be ascribed to symmetric stretching vibrations of nitrile groups and asymmetric stretching vibrations of C-O bonds, respectively. In the case of QPPESEN-2, the characteristic broad absorption signals at ~3393 cm<sup>-1</sup> can be assigned to -OH bonds and the peaks at 1685 cm<sup>-1</sup> can be attributed to the vibrational mode of C-N bonds. Both FT-IR and <sup>1</sup>H NMR spectra confirmed the successful preparation of QPPESEN-*x* AEMs.

## IEC, WU and SR of QPPESEN-*x* AEMs

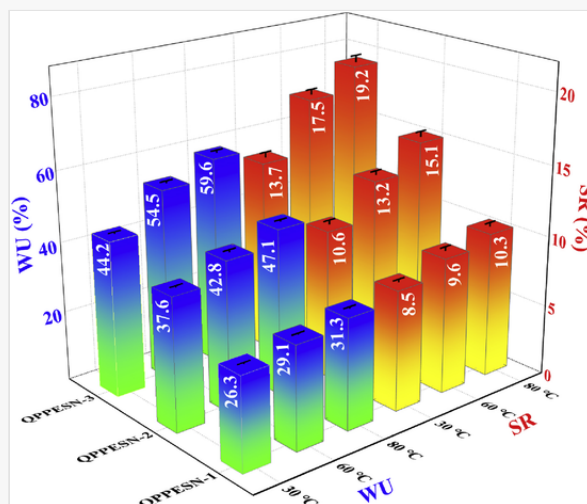
IEC reflects the concentration of exchangeable ion groups in membranes, which significantly influences the ionic conductivity of AEMs. The theoretical IECs can be calculated from the copolymer structure, assuming that the benzyl bromide groups are totally reacted with TMHQA groups and Br<sup>-</sup> are exchanged for OH<sup>-</sup>. The experimental IECs were estimated by back-titration method. As shown in Table 1, the experimental IECs ranged from 1.37 to 2.12 meq g<sup>-1</sup>, which are lower than the corresponding theoretical IECs. The discrepancy between experimental and theoretical values can be ascribed to the incomplete quaternization, which is caused by high steric hindrance effects of the long alkylene chains and phenolphthalein groups in hydrophilic segments.

Water molecules can act as ion carriers for OH<sup>-</sup> transport in AEMs and thus play a critical role in improving ionic conductivity. However, excessive water uptake induces severe swelling and leads to inferior mechanical strength. Thus, maintaining a suitable level of water uptake in AEMs is crucial for both desirable mechanical strength and high ionic conductivity of AEMs. As shown in Fig. 1, both WU and SR of QPPESEN-*x* AEMs raised with increasing temperature and IEC. For instance, the WU increased from 26.3% to 44.2% at 30 °C

and 31.3%–59.6% at 80 °C for QPPESN-1 to QPPESN-3, whereas the corresponding SR raised from 8.5% to 13.7% at 30 °C and 10.3%–19.2% at 80 °C. The AEMs with higher IEC values tend to be more hydrophilic and thus higher water uptake. The hydrated number ( $\lambda$ ) was also calculated to compare the water uptake among various membranes. As listed in Table 1,  $\lambda$  for QPPESN-*x* ranged from 10.7 to 11.6 at 30 °C and 12.7 to 15.6 at 80 °C.

alt-text: Fig. 1

Fig. 1

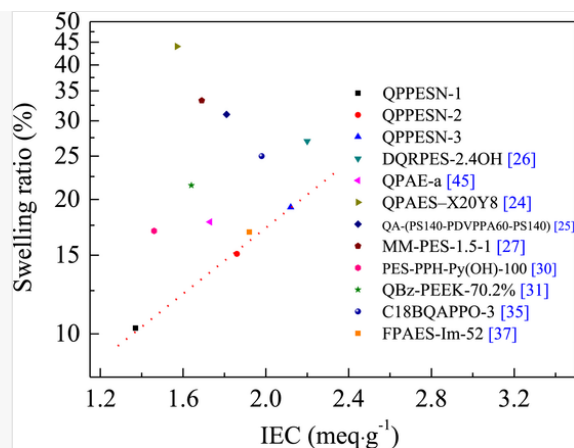


WU and SR of QPPESN-*x* AEMs at different temperatures.

The relationship between swelling ratio (80 °C) and IEC values of QPPESN-*x* with the main-chain type AEMs, such as DQPES-2.4OH (random) [26], QPAE-a (random) [45], QPAES-X20Y8 (block) [24], QA-(PS140-PDVPPA60-PS140) (block) [25], MM-PES-1.5-1 (block) [27] and side-chain type AEMs, such as PES-PPH-Py(OH)-100 [30], QBz-PEEK-70.2% [31], C18BQAPPO-3 [35] and FPAES-Im-52 [37] is presented in Fig. 2. The QPPESN-*x* membrane with a similar level of IEC exhibited a much lower swelling ratio, which demonstrates the as-prepared AEMs possess high dimensional stability and anti-swelling properties. It can be due to the introduction of phenolphthalein and nitrile groups in copolymers (Scheme 3). The rigid and bulky cardo groups on phenolphthalein units could force chains apart and generate additional interchain spacing, which is beneficial for storage of water molecules. Meanwhile, the nitrile groups with strong polarity could strengthen the intra/interchain interaction and restrict the membrane swelling [43,44].

alt-text: Fig. 2

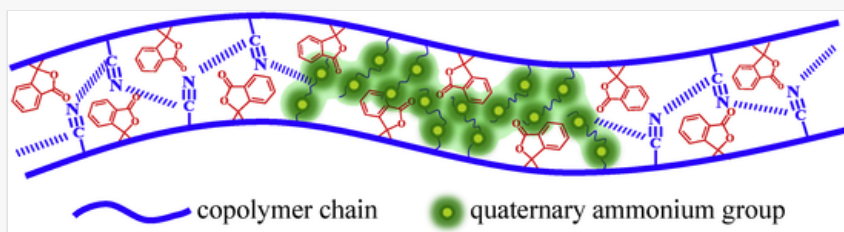
Fig. 2



Swelling ratio of QPPESN-*x* and previously reported membranes as a function of IEC at 80 °C.

alt-text: Scheme 3

Scheme 3



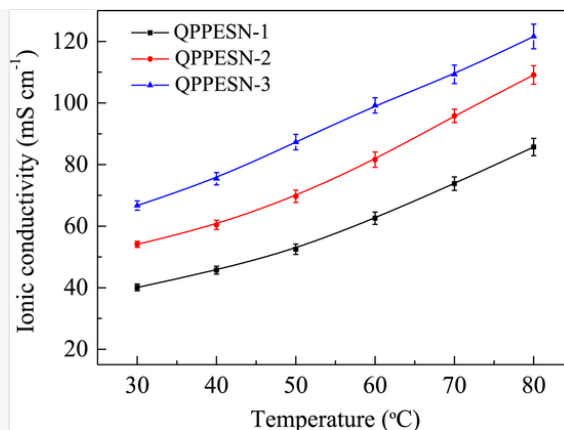
The schematic structure of QPPESN-*x* membranes.

## Ionic conductivity and morphology study

The ionic conductivity of QPPESN-*x* membranes at various temperatures is presented in Fig. 3. In the given temperature range, QPPESN-*x* AEMs exhibited high ionic conductivity above 10 mS cm<sup>-1</sup>, which is a critical requirement for fuel cell application [46]. Moreover, the hydroxide conductivity increased with increasing temperature as a result of improved ionic migration and water diffusion. In addition, when the ionic string content is increased (QPPESN-1 to QPPESN-3), the hydroxide conductivity increased from 40.1 to 66.7 mS cm<sup>-1</sup> at 30 °C and 85.7 to 121.6 mS cm<sup>-1</sup> at 80 °C owing to the higher IEC and WU. To study the ion conduction of QPPESN-*x* in detail, the conductivity data have been presented in the form of Arrhenius plot and apparent activation energy (*E<sub>a</sub>*) is calculated. As shown in Fig. S6 (Supporting information), *E<sub>a</sub>* of QPPESN-*x* membranes decreased with increasing ionic string content and ranged from 13.86 to 11.45 kJ mol<sup>-1</sup>. Moreover, the *E<sub>a</sub>* values of QPPESN-*x* membranes are much lower than the reported block-type membranes [26,28].

alt-text: Fig. 3

Fig. 3

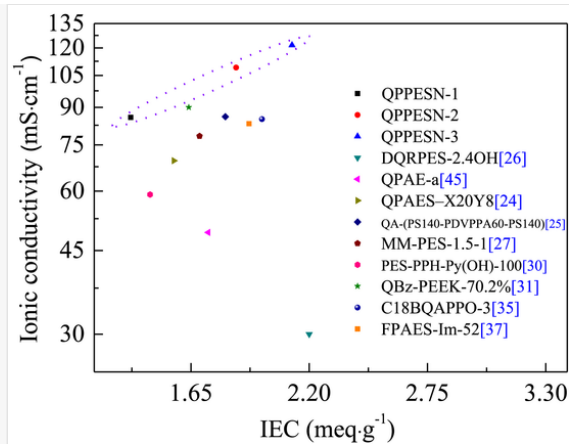


The ionic conductivity of QPPESN-*x* membranes at various temperatures.

Furthermore, QPPESN-*x* membranes are found to possess higher ionic conductivity at similar levels of IEC. [Fig. 4](#) compares the ionic conductivity (80 °C) of QPPESN-*x* with some recently reported AEMs as a function of IEC. It can be readily observed that QPPESN-*x* membranes render higher ionic conductivity at similar levels of IEC values. Similar phenomenon has also been observed in the comparison of conductivity and WU of the AEMs, as shown in [Fig. S7](#) (Supporting information). This can be ascribed to the formation of interconnected ionic transport channels from the well-defined microphase-separated structure, as demonstrated by AFM. As shown in [Fig. 5](#), the dark and cluster-like areas in the AFM images correspond to the water-contained hydrophilic phase, and the corresponding bright areas represent the hydrophobic phase of copolymer backbones [25]. It can be readily observed that QPPESN-*x* membranes displayed clear hydrophilic/hydrophobic phase-separated morphologies originated from the multiblock and flexible side-chain structures ([Scheme 3](#)). When the ionic string content increased, the quaternary ammonium groups on the flexible side chains of TMHQA tend to concentrate and aggregate, resulting in larger ionic domains. Thus, QPPESN-3 exhibited more pronounced ionic domains and superior microphase separation ability to QPPESN-1. Consequently, larger and abundant inter-connection-transport channels have been formed, which are highly desirable for OH<sup>-</sup> transport, resulting in a lower activation energy and higher conductivity. Therefore, it can be concluded that the proposed membrane design, consisting of flexible ionic strings grafted on the hydrophilic segments together with the phenolphthalein and nitrile groups, which are suspended on the backbones of multiblock copolymers, can effectively enhance ionic conductivity and retain dimensional stability of AEMs.

alt-text: Fig. 4

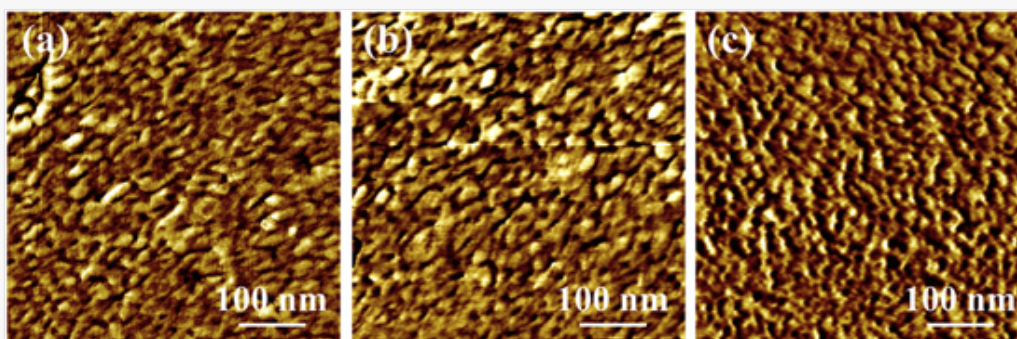
Fig. 4



Ionic conductivity of QPPESN-*x* and previously reported membranes as a function of IEC at 80 °C.

alt-text: Fig. 5

Fig. 5




AFM phase images of (a) QPPESN-1 (b) QPPESN-2 and (c) QPPESN-3 membranes.

## Mechanical characterization and thermal stability

The mechanical properties of AEMs are also considered for practical applications. As listed in Table 2, QPPESN-*x* membranes exhibited a tensile strength of 37.1–29.3 MPa and tensile elongation of 13.6–10.5% at 25 °C under 60% RH. Both tensile strength and elongation decreased with increasing IEC values, which can be explained by higher WU and SR of QPPESN-*x* membranes at higher levels of IEC. The water molecules in the membranes can render a plastic effect and restrain the mechanical properties [47].

alt-text: Table 2

Table 2

 The presentation of Tables and the formatting of text in the online proof do not match the final output, though the data is the same. To preview the actual presentation, view the Proof.

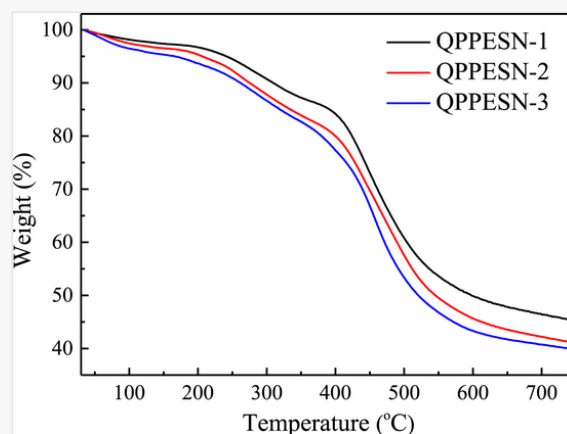
Mechanical properties of QPPESN-*x* membranes.

Membrane	Tensile strength (MPa)	Elongation at break (%)
QPPESN-1	37.1 ± 0.6	13.6 ± 0.4
QPPESN-2	33.8 ± 0.5	12.5 ± 0.3
QPPESN-3	29.3 ± 0.5	10.5 ± 0.3

As shown in Fig. 6, the thermal stability of QPPESN-*x* (OH<sup>-</sup> form) was evaluated by TGA under N<sub>2</sub> atmosphere. The QPPESN-*x* membranes exhibited three distinct thermal degradation stages: (1) the 1st weight loss occurred in the range of 30–200 °C, which can be due to the evaporation of bonded water; (2) the 2nd weight loss has been observed from 200 to 400 °C, which can be attributed to the degradation of quaternary ammonium groups; and (3) the 3rd weight loss occurred above 400 °C, which can be assigned to the cleavage of backbones. Furthermore, the 1st and 2nd weight loss fractions of QPPESN-*x* are approximately equal to the content of ionic strings in the membrane matrix. In general, QPPESN-*x* membranes exhibited excellent thermal stability below 200 °C.

alt-text: Fig. 6

Fig. 6



TGA curves of QPPESN-*x* membranes.

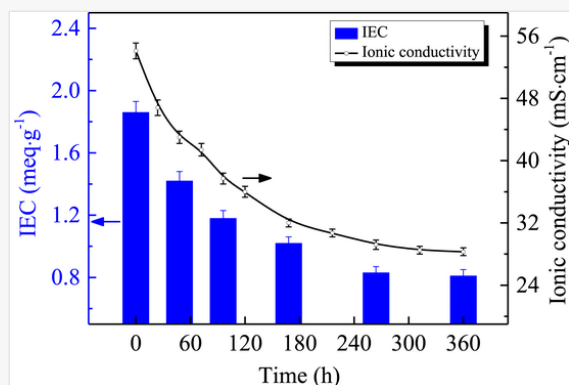
## Alkaline stability

The alkaline stability of as-prepared AEMs was investigated by soaking QPPESN-2 membrane in 80 °C KOH aqueous solution (1 mol L<sup>-1</sup>) and measuring the changes in ionic conductivity and IEC. As shown in Fig. 7, QPPESN-2 membrane retained ~52% (28.3 mS cm<sup>-1</sup>) of the initial ionic conductivity after being immersed for 360 h, whereas the corresponding IEC decreased from 1.86 to 0.81 meq g<sup>-1</sup>. This can be attributed to the decomposition of quaternary ammonium cation on TMHQA under alkaline conditions, which may be caused by Hofmann elimination and nucleophilic substitution [40,41]. Furthermore, the low hydration levels of the as-

prepared AEMs (Table 1) may be also partly responsible for the low stability. Recent researches showed a major degradation of materials (both at molecular levels as well as ionomeric levels) while tested at low hydration levels as compared to the high hydration levels in the alkaline environment [48–51]. However, the alkaline stability of as-prepared AEMs can be further improved. For instance, Shahi et al. [41] have reported that AEMs, with the same functionality but longer alkyl chain length on quaternary ammonium groups, exhibit better alkaline stability. Moreover, it has been found that methyl-based quaternary ammonium groups show much higher stability than ethyl-based QAs (regardless if it is mono, di, or tri ethyl) [49–51]. Recently, it has been also reported that AEMs bearing N-spirocyclic quaternary ammonium cations, e.g., pyrrolidinium and piperidinium cations, demonstrate superior alkaline stability [52–54]. These studies can serve as a baseline to improve the alkaline stability of as-prepared QPPESN-x membranes in future work.

alt-text: Fig. 7

Fig. 7



Alkaline stability of QPPESN-2 in 80 °C KOH aqueous solution (1 mol L<sup>-1</sup>).

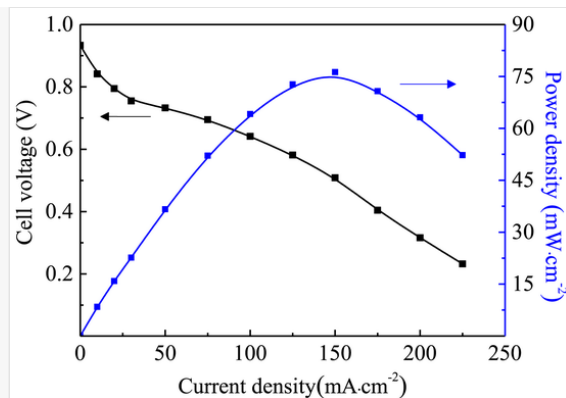
## Single cell performance

The QPPESN-2 membrane was chosen as a typical candidate for the MEA preparation and H<sub>2</sub>/O<sub>2</sub> single cell test. As shown in Fig. 8, an open circuit voltage (OCV) of 0.93 V and a maximum power density of 76.3 mW cm<sup>-2</sup> can be achieved for the single fuel cell under 100% RH at 80 °C. Furthermore, there is still room to enhance the single cell performance by optimizing the electrode architecture, MEA fabrication method and operating conditions [55,56]. Further work will focus on the optimization of these factors.

alt-text: Fig. 8

Fig. 8





A single H<sub>2</sub>/O<sub>2</sub> fuel cell performance using QPPESN-2 under 100% RH at 80 °C.

## Conclusions

In summary, a series of novel AEMs has been prepared by selectively grafting flexible ionic strings on phenolphthalein-based poly(arylene ether sulfone nitrile) multiblock copolymers. Owing to the high mobility and density of ionic strings on hydrophilic segments and the introduction of bulky phenolphthalein groups and strongly polar nitrile groups on hydrophobic segments, as-prepared QPPESN-*x* membranes rendered well-defined hydrophilic/hydrophobic microphase separation, resulting in the formation of inter-connected ion-transport channels and endowing anti-swelling properties. The IEC of QPPESN-*x* membranes ranged from 1.37 to 2.12 meq g<sup>-1</sup>, whereas the water uptake ranged from 26.3 to 44.2% at 30 °C and 31.3–59.6% at 80 °C. Correspondingly, the swelling ratio of QPPESN-*x* membranes ranged from 8.5 to 13.7% at 30 °C and 10.3–19.2% at 80 °C. Furthermore, QPPESN-*x* membranes rendered high hydroxide conductivity, ranging from 40.1 to 121.6 mS cm<sup>-1</sup> in the temperature of 30–80 °C, respectively, and superior ionic conductivity to IEC ratio at 80 °C. Moreover, the as-prepared QPPESN-*x* membranes exhibited desirable mechanical properties, excellent thermal stability below 200 °C and optimizable alkaline stability. A single H<sub>2</sub>/O<sub>2</sub> fuel cell using QPPESN-2 showed an open circuit voltage of 0.93 V and a peak power density of 76.3 mW cm<sup>-2</sup> at 80 °C. The current work presents an effective strategy of synthesizing high-conductivity AEMs, while the QPPESN-*x* membranes have the potential application for the AEM materials in AEMFCs. However, the controlled polymerization for the synthesis of block copolymers is still a challenge for the industrial production. Thus, our further work will focus on optimizing the synthetic process and alkaline stability of AEMs, MEA fabrication and fuel cell testing condition.


## Acknowledgments

This work is financially supported by the National Nature Science Foundation, China [Grant no. 21706032, 21701024], the Middle-aged and Young Teachers' Education Scientific Research Project of Fujian Province, China [Grant no. JAT170378], and the Scientific Research Foundation of Huaqiao University, China (Grant no. 605-50Y18020).

## Appendix A Supplementary data

Supplementary data to this article can be found online at <https://doi.org/10.1016/j.ijhydene.2019.11.090>.

## References

 The corrections made in this section will be reviewed and approved by journal production editor.

- [1] Zhang H, Shen PK. Recent development of polymer electrolyte membranes for fuel cells. *Chem Rev* 2012;112:2780–2832.
- [2] Moreno NG, Molina MC, Gervasio D, Robles JFP. Approaches to polymer electrolyte membrane fuel cells (PEMFCs) and their cost. *Renew Sustain Energy Rev* 2015;52:897–906.
- [3] Chandan A, Hattenberger M, El-kharouf A, Du S, Dhir A, Self V, et al. High temperature (HT) polymer electrolyte membrane fuel cells (PEMFC)–A review. *J Power Sources* 2013;231:264–278.
- [4] Peighambardoust SJ, Rowshanzamir S, Amjadi M. Review of the proton exchange membranes for fuel cell applications. *Int J Hydrogen Energy* 2010;35:9349–9384.
- [5] Scofield ME, Liu H, Wong SS. A concise guide to sustainable PEMFCs: recent advances in improving both oxygen reduction catalysts and proton exchange membranes. *Chem Soc Rev* 2015;44:5836–5860.
- [6] Merle G, Wessling M, Nijmeijer K. Anion exchange membranes for alkaline fuel cells: a review. *J Membr Sci* 2011;377:1–35.
- [7] Sheng W, Bivens AP, Myint M, Zhuang Z, Forest RV, Fang Q, et al. Non-precious metal electrocatalysts with high activity for hydrogen oxidation reaction in alkaline electrolytes. *Energy Environ Sci* 2014;7:1719–1724.
- [8] Lu S, Pan J, Huang A, Zhuang L, Lu J. Alkaline polymer electrolyte fuel cells completely free from noble metal catalysts. *Pnas* 2008;105:20611–20614.
- [9] Jang H, Hossain MA, Sutradhar SC, Ahmed F, Choi K, Ryu T, et al. Anion conductive tetra-sulfonium hydroxides poly(fluorenylene ether sulfone) membrane for fuel cell application. *Int J Hydrogen Energy* 2017;42:12759–12767.
- [10] Kim E, Lee S, Woo S, Park SH, Yim SD, Shin D, et al. Synthesis and characterization of anion exchange multi-block copolymer membranes with a fluorine moiety as alkaline membrane fuel cells. *J Power Sources* 2017;359:568–576.
- [11] Oh BH, Kim AR, Yoo DJ. Profile of extended chemical stability and mechanical integrity and high hydroxide ion conductivity of poly(ether imide) based membranes for anion exchange membrane fuel cells. *Int J Hydrogen Energy* 2019;44:4281–4292.

- [12] Arges CG, Wang L, Parrondo J, Ramani V. Best practices for investigating anion exchange membrane suitability for alkaline electrochemical devices: case study using quaternary ammonium poly(2,6-dimethyl 1,4-phenylene)oxide anion exchange membranes. *J Electrochem Soc* 2013;160:1258–1274.
- [13] Nykaza JR, Ye Y, Nelson RL, Jackson AC, Beyer FL, Davis EM, et al. Polymerized ionic liquid diblock copolymers: impact of water/ion clustering on ion conductivity. *Soft Matter* 2016;12:1133–1144.
- [14] Nakabayashi K, Sato Y, Isawa Y, Lo CT, Mori H. Ionic conductivity and assembled structures of imidazolium salt-based block copolymers with thermoresponsive segments. *Polymers* 2017;9:616.
- [15] Jheng LC, Tai CK, Hsu SL, Lin BY, Chen L, Wang BC, et al. Study on the alkaline stability of imidazolium and benzimidazolium based polyelectrolytes for anion exchange membrane fuel cells. *Int J Hydrogen Energy* 2017;42:5315–5326.
- [16] Kim S, Yang S, Kim D. Poly(arylene ether ketone) with pendant pyridinium groups for alkaline fuel cell membranes. *Int J Hydrogen Energy* 2017;42:12496–12506.
- [17] Xue B, Dong X, Li Y, Zheng J, Li S, Zhang S. Synthesis of novel guanidinium-based anion-exchange membranes with controlled microblock structures. *J Membr Sci* 2017;537:151–159.
- [18] Kwasny MT, Tew GN. Expanding metal cation options in polymeric anion exchange membranes. *J Mater Chem A* 2017;5:1400–1405.
- [19] Varcoe JR, Atanassov P, Dekel DR, Herring AM, Hickner MA, Kohl PA, et al. Anion-exchange membranes in electrochemical energy systems. *Energy Environ Sci* 2014;7:3135–3191.
- [20] Maurya S, Noh S, Matanovic I, Park EJ, Villarrubia CN, Martinez U, et al. Rational design of polyaromatic ionomers for alkaline membrane fuel cells with  $>1 \text{ W cm}^{-2}$  power density. *Energy Environ Sci* 2018;11:3283–3291.
- [21] Li N, Guiver MD. Ion transport by nanochannels in ion-containing aromatic copolymers. *Macromolecules* 2014;47:2175–2198.
- [22] Zeng L, Zhao TS. An effective strategy to increase hydroxide-ion conductivity through microphase separation induced by hydrophobic-side chains. *J Power Sources* 2016;303:354–362.
- [23] Liu L, Chu X, Liao J, Huang Y, Li Y, Ge Z, et al. Tuning the properties of poly(2,6-dimethyl-1,4-phenylene oxide) anion exchange membranes and their performance in  $\text{H}_2/\text{O}_2$  fuel cells. *Energy Environ Sci* 2018;11:435–446.
- [24] Li X, Liu Q, Yu Y, Meng Y. Synthesis and properties of multiblock ionomers containing densely functionalized hydrophilic blocks for anion exchange membranes. *J Membr Sci* 2014;467:1–12.

- [25] Zhu M, Zhang M, Chen Q, Su Y, Zhang Z, Liu L, et al. Synthesis of midblock-quaternized triblock copolystyrenes as highly conductive and alkaline-stable anion-exchange membranes. *Polym Chem* 2017;8:2074–2086.
- [26] Dong X, Lv D, Zheng J, Xue B, Bi W, Li S, et al. Pyrrolidinium-functionalized poly(arylene ether sulfone)s for anion exchange membranes: using densely concentrated ionic groups and block design to improve membrane performance. *J Membr Sci* 2017;535:301–311.
- [27] Kwon S, Rao AHN, Kim TH. Anion exchange membranes based on terminally crosslinked methyl morpholinium-functionalized poly(arylene ether sulfone)s. *J Power Sources* 2018;375:421–432.
- [28] Zhang X, Li S, Chen P, Fang J, Shi Q, Weng Q, et al. Imidazolium functionalized block copolymer anion exchange membrane with enhanced hydroxide conductivity and alkaline stability via tailoring side chains. *Int J Hydrogen Energy* 2018;43:3716–3730.
- [29] Arges CG, Li K, Zhang L, Kambe Y, Wu GP, Lwoya B, et al. Ionic conductivity and counterion condensation in nanoconfined polycation and polyanion brushes prepared from block copolymer templates. *Mol Syst Des Eng* 2019;4:365–378.
- [30] Gong F, Wang R, Chen X, Chen P, An Z, Zhang S. Facile synthesis and the properties of novel cardo poly(arylene ether sulfone)s with pendent cycloaminium side chains as anion exchange membranes. *Polym Chem* 2017;8:4207–4219.
- [31] Zhang Z, Xiao X, Yan X, Liang X, Wu L. Highly conductive anion exchange membranes based on one-step benzylation modification of poly(ether ether ketone). *J Membr Sci* 2019;574:205–211.
- [32] Lai AN, Zhuo YZ, Lin CX, Zhang QG, Zhu AM, Ye ML, et al. Side-chain-type phenolphthalein-based poly(arylene ether sulfone nitrile)s anion exchange membrane for fuel cells. *J Membr Sci* 2016;502:94–105.
- [33] Zhu Y, Ding L, Liang X, Shehzad MA, Wang L, Ge X, et al. Beneficial use of rotatable-spacer side-chains in alkaline anion exchange membranes for fuel cells. *Energy Environ Sci* 2018;11:3472–3479.
- [34] Wang C, Shen B, Xu C, Zhao X, Li J. Side-chain-type poly(arylene ether sulfone)s containing multiple quaternary ammonium groups as anion exchange membranes. *J Membr Sci* 2015;492:281–288.
- [35] He Y, Si J, Wu L, Chen S, Zhu Y, Pan J, et al. Dual-cation comb-shaped anion exchange membranes: structure, morphology and properties. *J Membr Sci* 2016;515:189–195.
- [36] Wei H, Li Y, Wang S, Tao G, Wang T, Cheng S, et al. Side-chain-type imidazolium-functionalized anion exchange membranes: the effects of additional hydrophobic side chains and

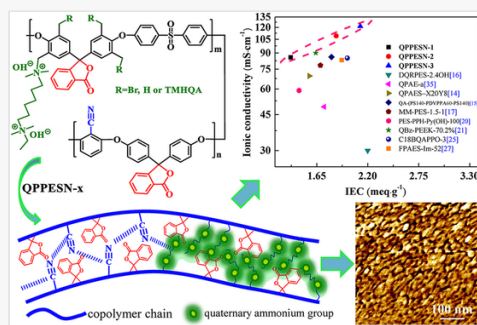
their hydrophobicity. *J Membr Sci* 2019;579:219–229.

- [37] Shen B, Pu H. Fluorene-containing poly(arylene ether sulfone)s with imidazolium on flexible side chains for anion exchange membranes. *Int J Hydrogen Energy* 2019;44:11057–11065.
- [38] Guo D, Lai AN, Lin CX, Zhang QG, Zhu AM, Liu QL. Imidazolium-functionalized poly(arylene ether sulfone) anion exchange membranes densely grafted with flexible side chains for fuel cells. *ACS Appl Mater Interfaces* 2016;8:25279–25288.
- [39] Lee WH, Mohanty AD, Bae C. Fluorene-based hydroxide ion conducting polymers for chemically stable anion exchange membrane fuel cells. *ACS Macro Lett* 2015;4:453–457.
- [40] He Y, Zhang J, Liang X, Shehzad MA, Ge X, Zhu Y, et al. Achieving high anion conductivity by densely grafting of ionic strings. *J Membr Sci* 2018;559:35–41.
- [41] Shukla G, Shahi VK. Well-designed mono- and di-functionalized comb-shaped poly(2,6-dimethylphenylene oxide) based alkaline stable anion exchange membrane for fuel cells. *Int J Hydrogen Energy* 2018;43:21742–21749.
- [42] Dang HS, Jannasch P. High-performing hydroxide exchange membranes with flexible tetra-piperidinium side chains linked by alkyl spacers. *ACS Appl Energy Mater* 2018;1:2222–2231.
- [43] Lai AN, Wang LS, Lin CX, Zhuo YZ, Zhang QG, Zhu AM, et al. Phenolphthalein-based poly(arylene ether sulfone nitrile)s multiblock copolymers as anion exchange membranes for alkaline fuel cells. *ACS Appl Mater Interfaces* 2015;7:8284–8292.
- [44] Shin DW, Lee SY, Lee CH, Lee KS, Park CH, McGrath JE, et al. Sulfonated poly(arylene sulfide sulfone nitrile) multiblock copolymers with ordered morphology for proton exchange membranes. *Macromolecules* 2013;46:7797–7804.
- [45] Li X, Liu Q, Yu Y, Meng Y. Quaternized poly(arylene ether) ionomers containing triphenyl methane groups for alkaline anion exchange membranes. *J Mater Chem A* 2013;1:4324–4335.
- [46] Li N, Zhang Q, Wang C, Lee YM, Guiver MD. Phenyltrimethylammonium functionalized polysulfone anion exchange membranes. *Macromolecules* 2012;45:2411–2419.
- [47] Dhakal HN, Zhang ZY, Richardson MOW. Effect of water absorption on the mechanical properties of hemp fibre reinforced unsaturated polyester composites. *Compos Sci Technol* 2007;67:1674–1683.
- [48] Diesendruck CE, Dekel DR. Water-a key parameter in the stability of anion exchange membrane fuel cells. *Curr Opin Electrochem* 2018;9:173–178.
- [49] Dekel DR, Amar M, Willdorf S, Kosa M, Dhara S, Diesendruck CE. Effect of water on the stability of quaternary ammonium groups for anion exchange membrane fuel cell applications. *Chem Mater* 2017;29:4425–4431.

- [50] Dekel DR, Willdorf S, Ash U, Amar M, Pusara S, Dhara S, et al. The critical relation between chemical stability of cations and water in anion exchange membrane fuel cells environment. *J Power Sources* 2018;375:351–360.
- [51] Willdorf-Cohen S, Mondal AN, Dekel DR, Diesendruck CE. Chemical stability of poly(phenylene oxide)-based ionomers in an anion exchange-membrane fuel cell environment. *J Mater Chem A* 2018;6:22234–22239.
- [52] Ponce-Gonzalez J, Whelligan DK, Wang L, Bance-Soualhi R, Wang Y, Peng Y, et al. High performance aliphatic-heterocyclic benzyl-quaternary ammonium radiation-grafted anion-exchange membranes. *Energy Environ Sci* 2016;9:3724–3735.
- [53] Lee N, Duong DT, Kim D. Cyclic ammonium grafted poly (arylene ether ketone) hydroxide ion exchange membranes for alkaline water electrolysis with high chemical stability and cell efficiency. *Electrochim Acta* 2018;271:150–157.
- [54] Pham TH, Olsson JS, Jannasch P. Poly(arylene alkylene)s with pendant N-spirocyclic quaternary ammonium cations for anion exchange membranes. *J Mater Chem A* 2018;6:16537–16547.
- [55] Pan ZF, An L, Zhao TS, Tang ZK. Advances and challenges in alkaline anion exchange membrane fuel cells. *Prog Energy Combust Sci* 2018;66:141–175.
- [56] Dekel DR. Review of cell performance in anion exchange membrane fuel cells. *J Power Sources* 2018;375:158–169.

## Graphical abstract

alt-text: Image 1



---

## Highlights

- High-performance AEMs were prepared by grafting ionic strings on multiblock copolymers.
  - Effect of the ionic strings content on AEMs' morphology and properties was studied.
  - The AEMs showed high ionic conductivity in the range of 40.1–121.6 mS cm<sup>-1</sup>.
  - Good anti-swelling properties and superior conductivity to IEC ratio were achieved at 80 °C.
- 

## Appendix A Supplementary data

The following is the Supplementary data to this article:

[Multimedia Component 1](#)

### Multimedia component 1

alt-text: Multimedia component 1

## Queries and Answers

**Query:** Your article is registered as a regular item and is being processed for inclusion in a regular issue of the journal. If this is NOT correct and your article belongs to a Special Issue/Collection please contact [d.norman@elsevier.com](mailto:d.norman@elsevier.com) immediately prior to returning your corrections.

**Answer:** Yes

**Query:** Please confirm that given names and surnames have been identified correctly and are presented in the desired order and please carefully verify the spelling of all authors' names.

**Answer:** Yes

**Query:** Please confirm that the provided email “[aonanlai@hqu.edu.cn](mailto:aonanlai@hqu.edu.cn)” is the correct address for official communication, else provide an alternate e-mail address to replace the existing one, because private e-mail addresses should not be used in articles as the address for communication.

**Answer:** Yes. “[aonanlai@hqu.edu.cn](mailto:aonanlai@hqu.edu.cn)” is the correct address for official communication.

**Query:** Have we correctly interpreted the following funding source(s) and country names you cited in your article: National Nature Science Foundation, China?

**Answer:** Yes